ELSEVIER

Surface Science 479 (2001) 183–190

SURFACE SCIENCE

www.elsevier.nl/locate/susc

Tip effects in the scanning-tunneling microscopy of semiconductor electrodes

R. Hiesgen [a], D. Meissner [b], W. Schmickler [c,*]

[a] *Physikdepartment E 19, Technische Universität München, D-85748 Garching, Germany*
[b] *Physikalische Chemie, Technische Universität Linz, A-4040 Linz, Austria*
[c] *Abteilung Elektrochemie Universität Ulm, D-89069 Ulm, Germany*

Received 6 October 2000; accepted for publication 7 February 2001

Abstract

The surface properties of a WSe_2 electrode have been investigated with a scanning-tunneling microscope in an electrochemical cell. Current–potential curves have been obtained for various electrode potentials and tunneling distances. They show a strong influence of the tip on the local electrode potential. The main features can be understood within a simple model describing the distribution of the electrostatic potential and its effect on the local electronic density.

Keywords: Electrochemical methods; Scanning tunneling microscopy; Solid–liquid interfaces; Semiconductor–electrolyte interfaces; Semi-empirical models and model calculations

1. Introduction

The scanning-tunneling microscope (STM) has been used with great success for the study of electrode surfaces. While most investigations have been performed on metal electrodes, a sizable amount of work has also been done on semiconductors – for recent reviews see Refs. [1,2]. Several authors have observed that the STM does not always serve as an unobtrusive tool, but that the tip potential seems to influence the electronic density on the semiconductor surface. However, a detailed investigation of this effect has been missing so far.

We have therefore measured electron tunneling from the van der Waals surface of a WSe_2 electrode to the tip of an STM, and systematically varied the system parameters such as tunneling bias, electrode potential and tunneling distance. Our results do indeed show a strong effect of the tip potential on the local electronic density on the electrode surface; they can be explained by a simple, Gouy–Chapman type model for the distribution of the electrostatic potential in the vicinity of the tip, combined with current ideas about the distance dependence of electron tunneling through water.

In vacuum science it is well established that the STM can effect the band bending at semiconductor surfaces with a low defect density [3,4]. In a recent

* Corresponding author. Tel.: +49-731-502-5402; fax: +49-731-502-5409.

E-mail addresses: rhiesgen@ph.tum.de (R. Hiesgen), dieter.meissner@jk.uni-linz.ac.at (D. Meissner), wolfgang.schmickler@chemie.uni-ulm.de (W. Schmickler).

0039-6028/01/$ - see front matter
PII: S0039-6028(01)00976-1

communication Sommerhalter et al. [5] have developed a one-dimensional model for the profile of the electrostatic potential at the surface of such semiconductors, and found good agreement with their experimental data. However, in an electrochemical cell the situation is more complicated, since two potential differences, the tunneling bias and the electrode potential, can be varied independently. So these results for the vacuum cannot be transferred to the electrochemical case.

2. Experimental

A detailed description of the experiments is given elsewhere [6,7]; we briefly report the important points in order to make this paper self-contained. The experiments were performed with a commercial STM (Nanoscope III, Digital Instruments, Santa Barbara, CA), which is equipped with a bipotentiostat. A platinum wire was used as a counter electrode and a AgCl-covered silver wire as a reference electrode. All potentials are given on the Ag/AgCl scale (223 mV vs. NHE) unless stated otherwise. The measurements were performed in an aqueous solution of 0.01 M H_2SO_4. The STM was operated in a closed chamber where the atmosphere can be maintained free of oxygen. As tunneling tips electrochemically etched Pt:Ir (90:10) wires have been used, which were insulated with an electrochemically applied lacquer in order to minimize the Faradaic currents [8].

2.1. Semiconductor

Monocrystalline n-WSe_2 samples with a doping level of 4×10^{16} cm^{-3} have been used as working electrodes. This layered semiconductor can be cleaved with adhesive tape so that large terraces of non-reactive van der Waals surfaces are exposed, which are separated by steps that are only a few monolayers high. These flat surface have a very low density of surface states [9,10]. WSe_2 has an indirect bandgap of 1.2 eV. In the dark the flat-band potential has a value of $\phi_{FB} = -200 \pm 50$ mV vs. Ag/AgCl independent of the pH [9]. Due to the layered crystal structure its properties are anisotropic and differ in the direction perpendicular to the layers (c-axis) and parallel. The dielectric constant has values of $\epsilon_{\|} = 4.18$ and $\epsilon_{\perp} = 12.7$ [11]. With the doping level mentioned above this results in a Debye length of about 50 nm for the direction perpendicular to the surface [12]. In the bulk, the lower edge of the conduction band is estimated to lie 0.1 eV above the Fermi level.

2.2. Current–potential curves

Current–potential curves were measured by an interrupted feedback method. Since our present set-up does not allow us to determine absolute values of the separation d between the tip and the substrate, relative values were defined in the following way: The electrode potential was set to a value of $\phi_{el} = -0.6$ V, the set-point potential, and for a given bias voltage a certain set-point current j_{sp} was chosen; different set-point currents correspond to different separations. Then the feedback control was switched off for a short period of time. During this period the semiconductor potential is changed to the desired value, and the resulting tunneling current is measured. Subsequently the feedback is switched on again to establish the distance control.

The value of the set-point potential is well below the flat-band potential, so that the tunneling current is large enough to ensure a stable tunneling regime. However, for different tip potentials the same set-point current results in different separations d. Our procedure also allows us to check that the STM tip does not touch the electrode surface: Even for the highest set-point current the tunneling current still depends strongly and non-linearly on the electrode potential, which indicates that there is no electric contact between tip and substrate.

The measuring time per point and the time for the feedback operation were both set to 0.3 s to establish a stationary tunneling current after the potential step. The distance change due to thermal drift during this period has been checked separately and is negligibly small. The current through the STM tip during the measuring time and the potential for every set of parameters were measured by two external voltmeters (Keithley 404) and stored in a separate computer. The residual

Faradaic current was measured at a bias voltage of 0 V, and subtracted from the measured tunneling current.

3. Theoretical considerations

For the electrolyte concentration employed the Debye length of the solution is of the order of 20 Å, and thus much larger than typical tunneling distances. Therefore it is to be expected that the tunneling bias will affect the electrostatic potential beneath the tip, as has been qualitatively discussed by Allongue [1]. On the other hand, the Debye length of the WSe_2 electrode is much larger than that of the solution, and its conductivity is comparatively negligible. So, to a good approximation, the potential in the vicinity of the tip will decay exponentially with $\exp(-\kappa r)$, where κ is the Debye inverse length of the solution, and r the distance from the tip. In order to describe the resulting distribution of the potential on the electrode surface, we introduce a cylindrical coordinate system with the origin on the surface and beneath the tip (see Fig. 1). Far from the tip, the potential will be equal to the applied electrode potential ϕ_{el}, measured with respect to an arbitrary reference electrode. Near the tip, it will decay from the tip value ϕ_{tip} to the limiting value ϕ_{el}. Therefore, within our model the distribution of electrostatic potential on the electrode surface is given by:

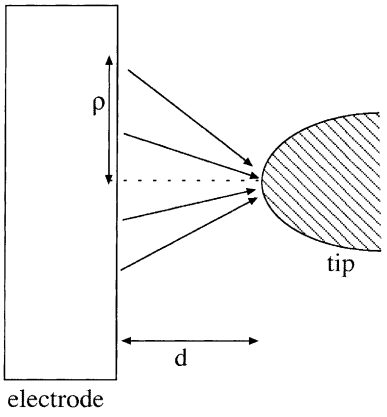

Fig. 1. Coordinate system employed for modeling the region between tip and electrode.

$$\phi(\rho) = (\phi_{tip} - \phi_{el}) \exp\left(-\kappa\sqrt{\rho^2 + d^2}\right) + \phi_{el} \quad (1)$$

where d is the separation between the tip and the electrode surface, and ρ is the radial distance of a point on the surface from the origin.

In order to obtain the rate of electron tunneling from the semiconductor to the tip we require the electronic density $n(\rho)$ at the surface, which is determined by the Fermi–Dirac distribution:

$$n(\rho) \propto \frac{1}{1 + \exp[(e_0\phi(\rho) - \phi_{deg})/kT]} \quad (2)$$

where ϕ_{deg} is the electrode potential at which the lower edge of the conduction band at the surface equals the Fermi level, and the surface becomes degenerate; e_0 is the unit of charge, T the temperature, and k Boltzmann's constant. For $e_0[\phi(\rho) - \phi_F] \gg kT$ the Fermi–Dirac distribution may be replaced by an exponential.

The contribution of a point with a cylindrical coordinate ρ on the electrode surface to the tunneling current is proportional to $n(\rho)$, and decays roughly exponentially with the distance from the tip [13]; we denote the corresponding decay parameter by β. The total tunneling current is then given by:

$$j \propto \int_0^\infty \rho \, d\rho \exp\left(-\beta\sqrt{\rho^2 + d^2}\right) n(\rho) \quad (3)$$

Eqs. (1)–(3) define our model. Obviously, in the derivation we have neglected minor effects like dipole potentials at the surface and non-linear Poisson–Boltzmann behavior. Also, in principal we should integrate over the electronic levels which contribute to the current; however, since the tunneling electrons come from a very narrow energy range this would only contribute a constant factor. We shall demonstrate below, that this simple model suffices for an understanding of our experimental data. In fact, without a detailed knowledge of the tip shape it will be difficult to improve our model substantially.

4. Results and discussion

A difficulty in the quantitative interpretation of the experimental data is the fact that the absolute value of the tip–electrode separation d is not known. For a given tip potential, different set-point currents give different separations, but for different tip potentials the same set-point current gives different separations. This has to be borne in mind during the following discussion.

The tip effects manifest themselves both in the distance dependence of the current, and in the shape of the current potential curves; we discuss the former dependence first. In the absence of tip effects the tunneling current would decay exponentially with distance and, for a given tip potential, the distance would be proportional to the logarithm of the set-point current. Hence a plot of the tunneling current vs. the logarithm of the set-point current should result in a straight line. However, in reality the corresponding plots display a marked curvature (see Fig. 2): At short distances (high set-point currents) the variation is much weaker than for large distances (low set-point currents). This behavior can easily be explained through the influence of the tip (see Fig. 3). At large distances the tip has little effect on the electrode surface, and then the current increases exponentially when the distance is reduced. However, at shorter distances the tip, whose potential is always more positive than that of the electrode, starts to raise the lower edge of the conduction band and thereby reduces the density of electrons on the surface; this effect partially compensates the increase of the current caused by the decrease of tunneling distance, and therefore the dependence becomes weaker. Of course, the effect of the tip and the band edges is limited to the region immediately beneath the tip.

These qualitative considerations are fully supported by explicit model calculations based on the equations presented in Section 2. All calculations were performed for a Debye length of $1/\kappa = 20$ Å for the solution, and a tunneling decay length of $1/\beta = 1$ Å, which seems to be a typical value for aqueous solutions [13]. Fig. 4 shows calculated curves for the distance dependence of the tunneling current. In line with the experimental curves they exhibit a marked increase of the slope at larger separations. This change in the slope implies an increase of the apparent barrier height with increasing separation; the same effect has also been observed in the vacuum [3].

The influence of the tip also affects the current–potential curves. In the absence of such effects we would expect the following behavior: When we

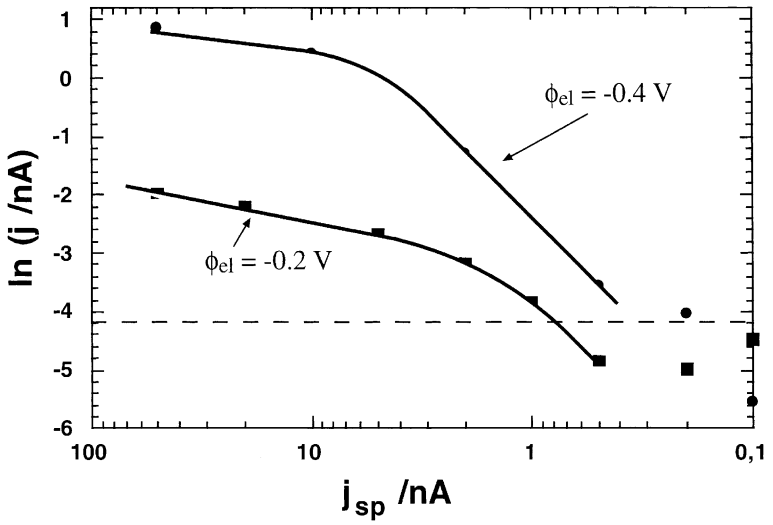

Fig. 2. Tunneling current as a function of the set-point current for two different electrode potentials: the tip potential was $\phi_{tip} = 0.2$ V in both cases. The dotted line represents the lower limit for which the current can be reliably measured.

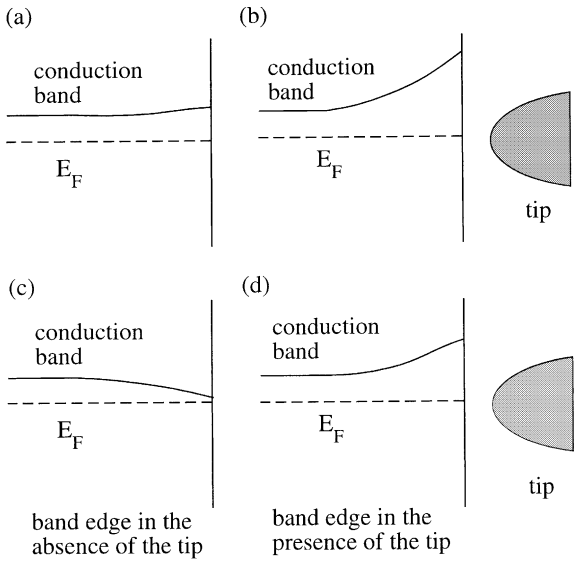

Fig. 3. Effect of the tip on the band bending near the surface for two different electrode potentials (schematic); the tip potential lies above the electrode potential. In (c) and (d) the electrode potential is lower than in (a) and (b).

scan the electrode potential from a value above the flat-band potential in the negative direction, the Fermi level of the electrode is raised, and the band-bending decreases – this corresponds to going from the situation in Fig. 3a towards that of Fig. 3c. Simultaneously, the density of electrons at the surface increases exponentially, and so does the tunneling current. This behavior continues until the electrode reaches the potential ϕ_{deg}, when the Fermi level touches the lower edge of the conduction band and the surface attains a metal-like conductivity. At this and at more negative potentials the tunneling electrons will mainly come from the Fermi level; in addition, the metal-like conductivity of the surface affects the distribution of the double-layer potential. This should result in a much weaker dependence of the tunneling current on the electrode potential. We note that surface defects should play no role, since the defect density of the van der Waals surfaces is known to be low, and the tunneling current comes from a small surface region only.

Fig. 5 shows a few plots of the current as a function of the electrode potential for various experimental parameters. Only for a tip potential of $\phi_{tip} = -0.2$ V does the current show a gradual change of the slope at more negative potentials. In all other cases the current increases exponentially over the whole measured range, indicating that the band edge beneath the tip is always above the Fermi level, and the electronic density increases exponentially as the band edge is lowered. Further investigation shows that this behavior is

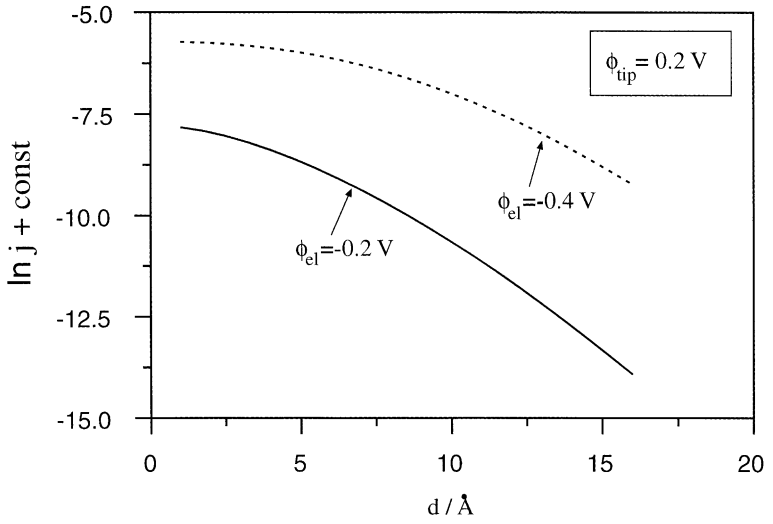

Fig. 4. Tunneling current as a function of the substrate–tip separation for a tip potential of $\phi_{tip} = 0.2$ V and two different electrode potentials (calculated curves).

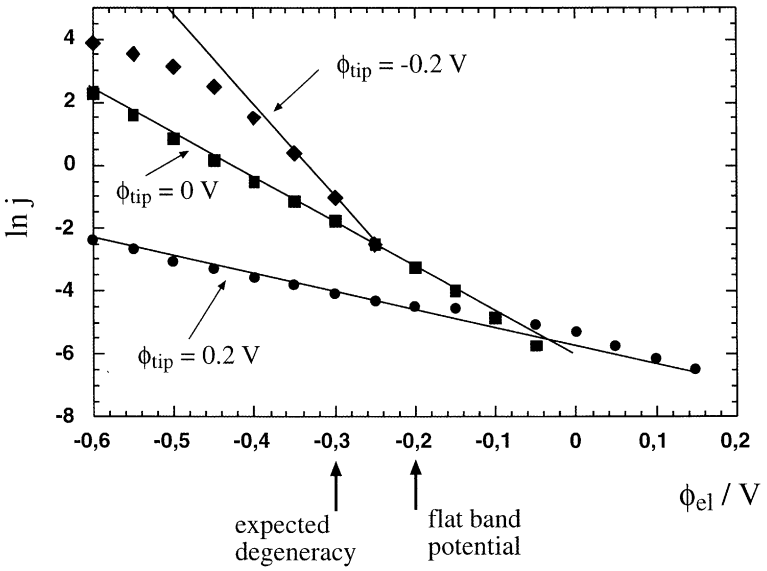

Fig. 5. A few examples of experimental current–potential curves.

symptomatic: The curves for tip potential of −0.2 V always show a distinct curvature (see Fig. 6a). This tip potential is only a little higher than the potential ϕ_{deg}, so that its influence does not prevent the surface from becoming degenerate. In contrast, current–potential curves for higher tip potentials obey an exponential dependence throughout (see Fig. 6b for examples). At these potentials the effect of the tip is sufficiently strong to prevent the tunneling region from becoming degenerate.

Again, this interpretation of the experimental results is supported by model calculations. Fig. 7 shows a few calculated plots of the current as a function of the electrode potential for a separation of $d = 6$ Å and several values of the tip potential. The curves for $\phi_{tip} = 0$ V to $\phi_{tip} = 0.4$ V show essentially an exponential dependence, just like the experimental data; even the slopes compare favorably. Only the curve for $\phi_{tip} = -0.2$ V, in line with the experimental curve, shows a distinct curvature as the band edge beneath the tip dips below the Fermi level.

Finally we note that the boundary conditions at the electrochemical interface are rather different from those in the vacuum. Typically, the solution is a much better conductor than the semiconducting electrode. Therefore a positive excess charge on the tip is screened by the solution, not by the electrode, and when this tip is very close to the surface it raises its potential. In contrast, in the vacuum an excess charge on the tip must be balanced by the charge on the semiconductor. This must borne in mind when comparing our results with those observed in the vacuum [4,5].

5. Concluding remarks

Our experimental results clearly demonstrate that the potential of the tip affects the local electrode potential. Such an effect has been suggested before, but our work is the first systematic investigation for an electrochemical system. The main features of our experiments can be understood within a simple model for the diffuse double layer combined with tunneling theory. For a more quantitative understanding it would be desirable to measure the tip-sample separation directly, and obtain current–potential curves at well-defined distances.

Qualitatively, tip-induced band bending discussed here is similar to that observed in the vacuum. However, in the electrochemical situation

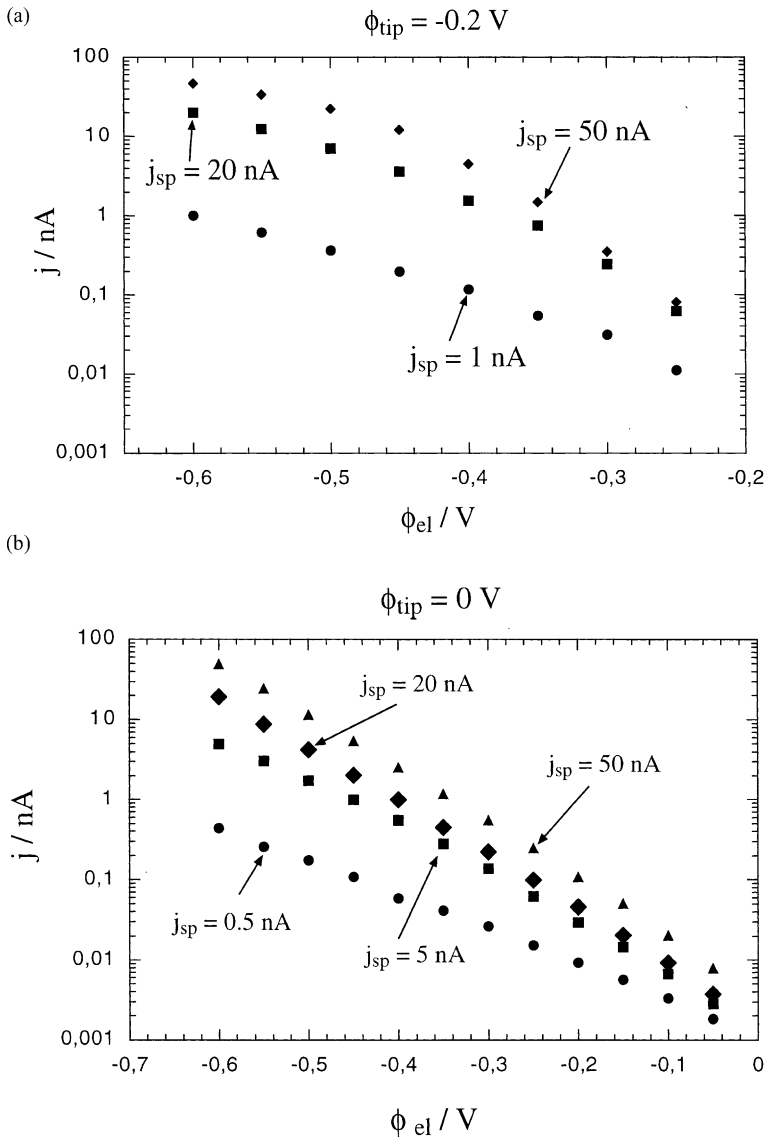

Fig. 6. Current–potential curves for several set-point currents j_{sp} and tip potentials of (a) $\phi_{tip} = -0.2$ V (b) and $\phi_{tip} = 0$ V.

this effect is stronger, because the potential drop over the solution is smaller. In addition, a one-dimensional model does not suffice because the electrode potential can be set independent of the tunneling bias, so that the electrostatic potential changes also in the direction parallel to the surface.

Such tip effects on electrode surfaces are not restricted to semiconductors, but have also been observed on metal electrodes. Well known examples are the shading of the electrode surface through the tip during metal deposition [14], and the local dissolution or deposition of metals at potentials at which they would not occur in the absence of the tip [15–17]. The boundary conditions at the metal–solution interface differ from those at semiconductor electrodes, so our model must be substantially modified for these systems.

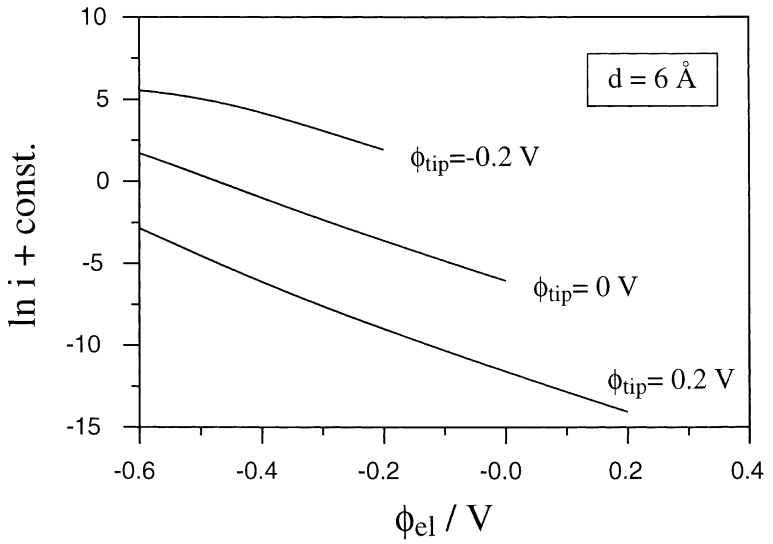

Fig. 7. Calculated tunneling current as a function of the electrode potential for a separation of $d = 6$ Å and for various tip potentials.

Finally we note that tip effects form the basis of the nanostructuring of electrode surfaces through the deposition of clusters or the creation of pits, and are thus potentially of great technological interest.

Acknowledgements

Financial support by the Deutsche Forschungsgemeinschaft is gratefully acknowledged.

References

[1] P. Allongue, in: H. Gerischer, C.E. Tobias (Eds.), Advances in Electrochemical Science and Engineering, Vol. 4, VCH, New York, 1995.
[2] K. Uosaki, M. Koinuma, S. Ye, in: A. Wieckowski (Ed.), Interfacial Electrochemistry, Marcel Dekker, New York, 1999.
[3] M. Weimer, J. Kramar, J.D. Bladeschwieler, Phys. Rev. B 39 (1989) 5572.
[4] M. McEllistream, G. Haase, D. Chen, R.J. Hamers, Phys. Rev. Lett. 70 (1993) 2471.
[5] C. Sommerhalter, T.W. Matthes, J. Boneberg, P. Leiderer, M.C. Lux-Steiner, J. Vac. Sci. Technol. B 15 (1997) 1876.
[6] R. Hiesgen, D. Meissner, J. Phys. Chem. 102 (1998) 6549.
[7] R. Hiesgen, M. Krause, D. Meissner, Electrochim. Acta 45 (2000) 3213.
[8] C.E. Bach, R.J. Nichols, W. Beckmann, H. Meyer, A. Schulte, J.O. Besenhard, P.D. Jannakoudakis, J. Electrochem. Soc. 140 (1993) 1281.
[9] C. Sinn, Ph.D. Thesis, University of Hamburg, 1989.
[10] W. Jaegermann, in: A. Aruchamy (Ed.), Photoelectrochemistry and Photovoltaics of Layered Semiconductors, Kluwer Academic Publishers, Dordrecht, 1992.
[11] A.R. Beals, W.Y. Liang, J. Phys. C: Solid State Phys. 9 (1976) 2459.
[12] R. Schlaf, A. Klein, C. Pettenkofer, W. Jaegermann, Phys. Rev. B 48 (1993) 14242.
[13] W. Schmickler, in: J. Lipkowski, P.N. Ross (Eds.), Imaging of Surfaces and Interfaces, Wiley, New York, 1999.
[14] U. Stimming, R. Vogel, J. Power Sources 43–44 (1993) 169.
[15] H. Nachara, S. Ye, K. Uosaki, Appl. Phys. A: Mater. Sci. Process. 66 (1998) S457.
[16] R. Ullmann, T. Will, D.M. Kolb, Ber. Bunsenges. Phys. Chem. 99 (1995) 1414.
[17] Z.X. Xie, D.M. Kolb, J. Electroanal. Chem. 481 (2000) 177.